ACS APPLIED MATERIALS & INTERFACES

Research Article

www.acsami.org

Monodisperse Boronate Polymeric Particles Synthesized by a Precipitation Polymerization Strategy: Particle Formation and Glycoprotein Response from the Standpoint of the Flory–Huggins Model

Jianxi Liu,[†,‡] Yanyan Qu,[†,‡] Kaiguang Yang,[†] Qi Wu,[†,‡] Yichu Shan,[†] Lihua Zhang,*[,†] Zhen Liang,[†] and Yukui Zhang[†]

[†]National Chromatographic R & A Center, Key Laboratory of Separation Science for Analytical Chemistry, Dalian Institute of Chemical Physics, Chinese Academy of Sciences, Dalian 116023, China

[‡]University of Chinese Academy of Sciences, Beijing 100049, China

Supporting Information

ABSTRACT: The development of a highly specific recognition system for glycoprotein capture from complex biological samples is a prerequisite to the success of mass spectra-based glycoproteomics analysis. To achieve this purpose, a one-pot precipitation polymerization (PP) strategy with a novel solvent system composed of water/ethanol (4:1, v/v) is described for preparing boronate-affinity polymeric micro/nano particles using 4-vinylphenylboronic acid (VPBA) as the functional monomer and *N*,*N*′-methylenebis(acrylamide) (MBA) alone or together with divinylbenzene (DVB) as the cross-linker(s). The proposed polymerization strategy not only affords monodisperse polymeric submicrometer particles with a smooth surface and controllable size, ranging from 300 to 700 nm, but also increases the loading capacity of boronic acid, which could hardly be achieved by other polymerization methods, thus leading to the specific recognition of glycoproteins. The effects of solvent systems and monomers on the morphology and boronate-affinity capacity of prepared materials were further investigated based on the Flory–Huggins model. It was proved that the reaction rate of various monomers during particle formation might be the key factor affecting the affinity capacity for glycoproteins. Our results demonstrated that under the theoretical guidance of the Flory–Huggins model the PP strategy with a selected monomer and solvent system might provide a good approach to prepare submicrometer polymer particles with plenty of boronic acid groups on the surface to achieve a highly selective enrichment of glycoproteins.

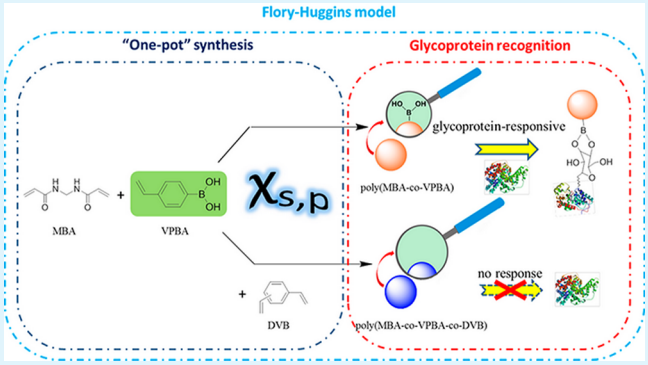

KEYWORDS: *one pot, polymerization, glycoprotein response, boronate affinity, Flory–Huggins model*

1. INTRODUCTION

Boronic acids are important ligands for the specific recognition of 1,2- and 1,3-cis-vicinal diol-containing biomolecules, such as saccharides,[1,2] nucleosides,[3] and glycoproteins.[4] The principle relies on the chemistry whereby five or six-membered cyclic esters are generated via covalent bonds between boronic acids and cis-diols in basic aqueous solution, whereas esters reversibly disassociate to release the receptor compound when the pH of the solution is changed to acidic.[5,6] With the in-depth study of proteomics, boronic acid-functionalized materials for glycoprotein enrichment have recently drawn increasing attention in glycoproteome analysis.

To date, several kinds of boronate-affinity materials, including magnetic or Au nanoparticles,[7−9] mesoporous silica,[10] carbon nanotubes,[11] and organic–inorganic hybrid nanoparticles,[12] have been prepared. However, most of them are synthesized by a postgrafting strategy, such as covalent modification or noncovalent interaction, which has the limitation of a low boronic acid-conjugation efficiency, and multistep synthesis under harsh conditions is used to modify boronic acid on solid surfaces. Recently, copolymerization has been employed as an alternative to postgrafting owing to its merits of high modification efficiency and facile manipulation.[13] Therefore, the synthesis of monodisperse bornoate polymer particles via copolymerization might be promising to achieve the highly specific recognition of glycoproteins.

4-Vinylphenylboronic acid (VPBA) is a commonly applied monomer that contains one boronic acid functional group for cis-diol-containing biomolecules isolation and one vinyl group for free-radical polymerization. Recent years have witnessed

Received: November 15, 2013
Accepted: January 14, 2014
Published: January 14, 2014

   dx.doi.org/10.1021/am405144x | ACS Appl. Mater. Interfaces 2014, 6, 2059−2066

growing interest on boronate particles functionalized with VPBA to achieve glycoprotein/peptide enrichment.[14−16] Shen et al. fabricated hybrid boronic acid-functionalized core−shell nanoparticles, SnO_2@poly (2-hydroxyethylmethacrylate-*co*-styrene-*co*-VPBA), by a hydroxyl-exchange reaction and subsequent radical polymerization.[14] Pan et al. prepared core−shell−shell-structured magnetic composite microspheres, Fe_3O_4@SiO_2@poly (methyl methacrylate-*co*-4-vinylphenylbornoic acid) (Fe_3O_4@SiO_2@P(MMA-*co*-VPBA)), by emulsion polymerization for glycoprotein enrichment.[15] Later, we synthesized boronate-functionalized polymer core−shell nanoparticles, poly(*N*,*N*′-methylenebis(acrylamide)-*co*-methacrylic acid)@VPBA (P(MBA-*co*-MAA)@(VPBA)), with the combined strategy of distillation precipitation polymerization (DPP) for core and radical polymerization for shell formation.[16] However, the limitations of preparing such core−shell architectures include the long consuming time and low modification yield resulting from the employed sophisticated multistep synthesis reactions, which involve washing the residual monomer, drying the core particles, and redispersing the cores in solvent with additional comonomer and initiator added for shell formation.

In comparison, one-pot synthesis strategies have drawn much attention owing to their high yield, facile manipulation, and fast preparation speed,[17,18] among which precipitation polymerization (PP) has shown its versatility for the preparation of submicrometer polymer particles. Although various particles have been prepared via PP,[19,20] few reports are available for the synthesis of monodisperse boronate submicrometer polymeric particles because of the difficulty in exploiting an appropriate solvent system to dissolve simultaneously the functional monomer, VPBA, with its comonomers for particle fabrication. Moreover, the effect of the interactions between various growing polymeric chains and solvent molecules on the precipitation process of particles as well as on glycoprotein capture has not been studied.

Herein, to the best of our knowledge, for the first time, we prepared boronate submicrometer polymeric particles with uniform size and shape by a facile and time-saving PP strategy using a novel solvent. Such particles were further applied to enrich glycoproteins. Meanwhile, the Flory−Huggins model was successfully employed to explore the correlation between the morphology and glycoprotein-capture response of the material with polymer−solvent interactions during the polymerization process.

2. EXPERIMENTAL SECTION

Reagents and Materials. Trypsin (bovine pancreas), horseradish peroxidase (HRP), urea (99.5%), methacrylic acid (MAA, 98%), *N*,*N*′-methylenebis(acrylamide) (MBA, 98%), divinylbenzene (DVB, technical grade, 80%), and 4-vinylphenylboronic acid (VPBA) were purchased from Sigma-Aldrich (St. Louis, MO). Bovine serum albumin (BSA, bovine serum) was obtained from Sino-American Biotec (Luoyang, China). Dithiothreitol (DTT) and iodoacetamide (IAA) were from Acros (Morris Plains, NJ). 2,2′-Azobisisobutyronitrile (AIBN) was purchased from Shanghai Fourth Reagent Plant (Shanghai, China) and recrystallized in our laboratory. SDS-PAGE gel (Br-PreGel, 4−15% Tris-HCl) was obtained from Sangon Biotech (Shanghai, China). Anhydrous ethanol (analytical reagent) was purchased from Tianjin Damao Chemical Reagent Factory (Tianjin, China). Water was purified by a Milli-Q system (Millipore, Milford, MA). All chemical reagents were used without further purification unless otherwise indicated.

Synthesis of VPBA-Containing Particles. The procedure to prepare P(MBA-*co*-VPBA) by a one-pot precipitation polymerization strategy was as follows. MBA (1.2 mmol), VPBA (0.2 mmol), and AIBN (2 wt % relative to the total monomer) were dissolved in 10 mL of water/ethanol (4:1, v/v) in a 25 mL round-bottomed flask. The polymerization solution was then purged with nitrogen for 10 min. Subsequently, the flask was submerged in an oil bath under magnetic stirring and heated at 70 °C, where it was maintained for 24 h. The resulting polymer particles were purified by centrifugation and suspension three times in water/ethanol (4:1, v/v) and then dried in a vacuum oven at room temperature. This procedure was repeated but with alteration of the volume ratio of water/ethanol, comonomer categories, and composition to prepare a series of VPBA-containing particles (i.e., P(MBA-*co*-DVB-*co*-VPBA)), with the total monomer amount of 0.14 mmol and 2 wt % AIBN relative to total comonomer amount.

Characterization. The morphology of the particles was observed by scanning electron microscopy (SEM) on a JSM-6360 LV (JEOL, Tokyo, Japan). The size distribution and zeta potential of the particles dispersed in water were measured on a Malvern Nano Z Zetasizer (Worcestershire, UK). Fourier-transform infrared spectra were acquired on a PerkinElmer Spectrum GX spectrometer (San Jose, CA) by mixing polymer particles with KBr and scanning in the range of 400−4000 cm^{-1}.

Glycoprotein Enrichment. P(VPBA-*co*-MBA) particles (1 mg) were suspended in 200 μL of glycoprotein solution (50 mM NH_4HCO_3, pH 9.0), incubated with shaking for 2 h at room temperature, and then centrifuged at 13 000 rpm for 10 min. After the supernatant was decanted, the deposit was rinsed repeatedly with NH_4HCO_3 buffer to remove the nonspecifically adsorbed proteins. Finally, 20 μL of solution, composed of ACN, H_2O, and TFA (50:49:1, v/v/v), was added to release the glycoproteins at room temperature for 1 h, and the supernatant was deposited on a MALDI plate directly after centrifugation at 13 000 rpm for 5 min. With the same protocol, P(MBA-*co*-DVB-*co*-VPBA) polymer particles were also applied for glycoprotein enrichment, and the evaluation of enrichment reproducibility and lifetime of P(VPBA-*co*-MBA) was also performed by this protocol.

Glycoprotein purification from egg white by P(MBA-*co*-VPBA) was also performed following a modified protocol. Briefly, egg white was first diluted 100-fold with 30% ACN (v/v) in 100 mM phosphate buffer (pH 9.0). Then, 2 mg of prepared boronate nanoparticles were suspended in 200 μL of egg white solution and incubated with shaking for 2 h at room temperature. After centrifugation to remove the supernatant, 100 mM acetate buffer (pH 2.7) containing 50% ACN (v/v) was applied to elute the captured glycoproteins. Finally, the eluent was dried by a Speed Vac concentrator (ThermoFisher, San Jose, CA) for SDS-PAGE analysis.

MS Analysis. MALDI-TOF MS was performed on an Ultraflex III TOF/TOF (Bruker Daltonics, Bremen, Germany). Sinapic acid (SA) matrix solution (20 mg mL^{-1}) was prepared in ACN/H_2O/TFA (60:40:1, v/v/v). Equivalent amounts (0.5 μL) of the sample and SA were sequentially dropped onto the MALDI plate for MS analysis. Spectra were obtained in positive ionization mode using linear detection.

Protein Adsorption Isotherms. Protein adsorption was performed with the binding buffer that contained 100 mM phosphate buffer (pH 9.0). P(MBA-*co*-VPBA) particles (1.5 mg) were incubated in 1 mL of protein samples with different concentrations (from 0.1 to 1 mg mL^{-1}) at room temperature for 3 h. Then, the suspension was centrifuged, and the protein concentration of the supernatant was measured by HPLC at regular intervals. The adsorption capacity (Q, mg g^{-1}) was calculated according to the the following equation

$$Q = \frac{(C_0 - C_t)V}{10^{-3}m}$$

where C_0 (mg mL^{-1}) is the initial protein concentration, C_t (mg mL^{-1}) is the supernatant protein concentration, V (mL) is the volume of protein solution, and m (mg) is the weight of the particle.

Scheme 1. (a) Synthesis of Submicrometer P(MBA-*co*-VPBA) and P(MBA-*co*-VPBA-*co*-DVB) Particles by a One-Pot PP Strategy and (b) Applications in the Selective Recognition of Glycoproteins

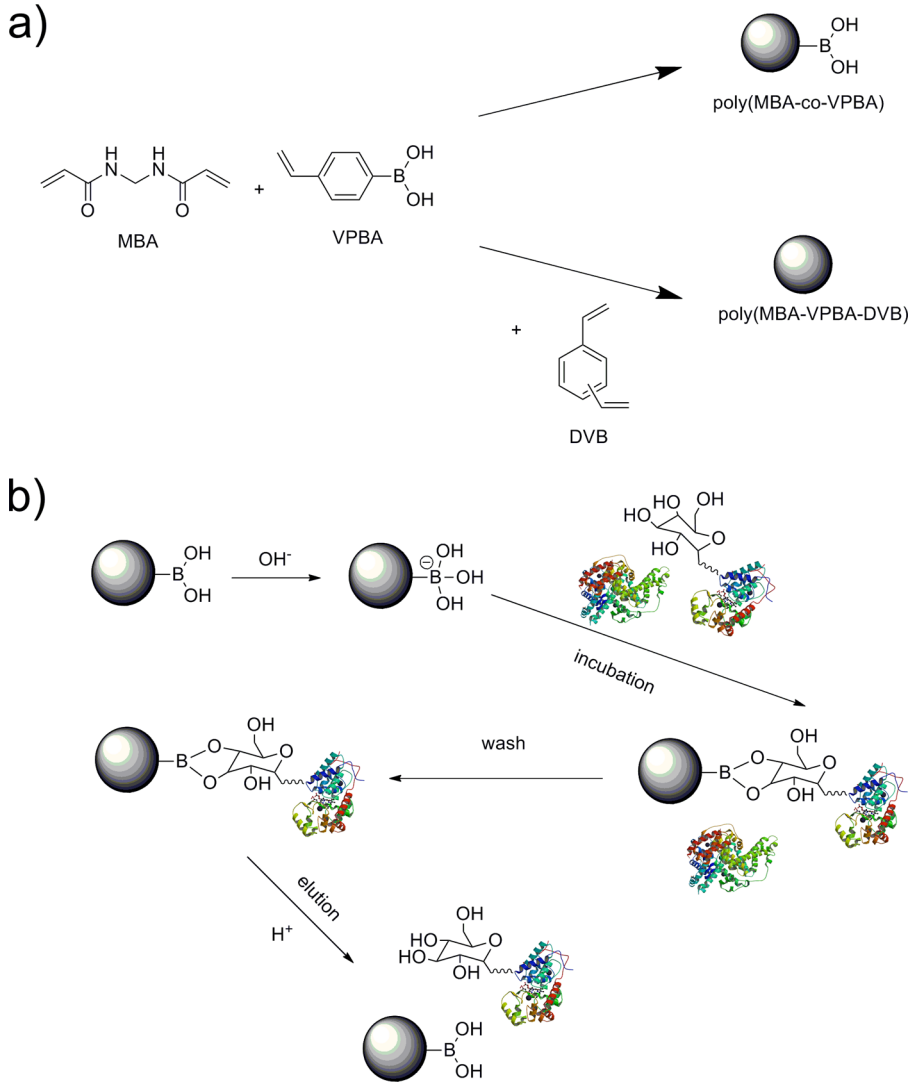

SDS-PAGE Analysis. Proteins were diluted 2-fold with 2× reducing sample buffer and then boiled at 100 °C for 3 min. Gel electrophoresis for protein separation was performed using a regular SDS-PAGE system according to the manufacturer's instructions (Bio-Rad, Hercules, CA). Gel contents were visualized with silver staining.

3. RESULTS AND DISCUSSION

Synthesis of Submicrometer P(MBA-*co*-VPBA) Particles by the PP Strategy. In contrast to traditional polymerization strategies, including suspension polymerization, emulsion polymerization, and dispersion polymerization, which always apply abundant dispersants, the polymerization system for PP requires no surfactant or steric stabilizers[21−23] and thus, after the enrichment of samples with the prepared particles, the disturbance of leaked dispersants on mass spectrometry-based detection could be avoided.[24] With its phenyl group, VPBA exhibited noticeable hydrophobic properties that might cause nonspecific adsorption towards nonglycoproteins. To increase the hydrophilicity of the prepared VPBA-functionalized polymer particles, we proposed a PP strategy to prepare submicrometer polymer particles with VPBA as the functional monomer and MBA as the hydrophilic cross-linker (Scheme 1a). Because of the different polarity of VPBA and MBA, the applied solvent system for polymerizaiton has remarkable effects on the morphology of the resulting polymer networks.[25,26] Therefore, it is crucial to choose an appropriate solvent system for the in situ formation of regular polymer particles with VPBA as the functional monomer.

Acetonitrile is a commonly used solvent in PP because its' Hansen's solubility parameter (HSP, 24.3 $MPa^{1/2}$) always meets the requirement for polymeric particle formation with various monomers.[25,27] However, in such a solvent, the functional monomer, VPBA, is hard to dissolve. As an alternative, water has been reported as the weak solvent for VPBA in copolymerization,[14] but the solubility was limited. Alcohols, such as methanol and ethanol, are good solvents for VPBA. The HSP of methanol (29.7 $MPa^{1/2}$) is similar to that of ethanol (26 $MPa^{1/2}$) and thus both of them are suitable for PP. With the consideration that ethanol is a kind of green solvent with low toxicity, it was employed as the representative alcohol in our work. However, when ethanol was used alone, our study showed that the growing polymeric chains resulted in the formation of gel instead of regular particles during the polymerization. Therefore, ethanol/water was chosen as the optimal solvent system in our following work.

dx.doi.org/10.1021/am405144x | ACS Appl. Mater. Interfaces 2014, 6, 2059−2066

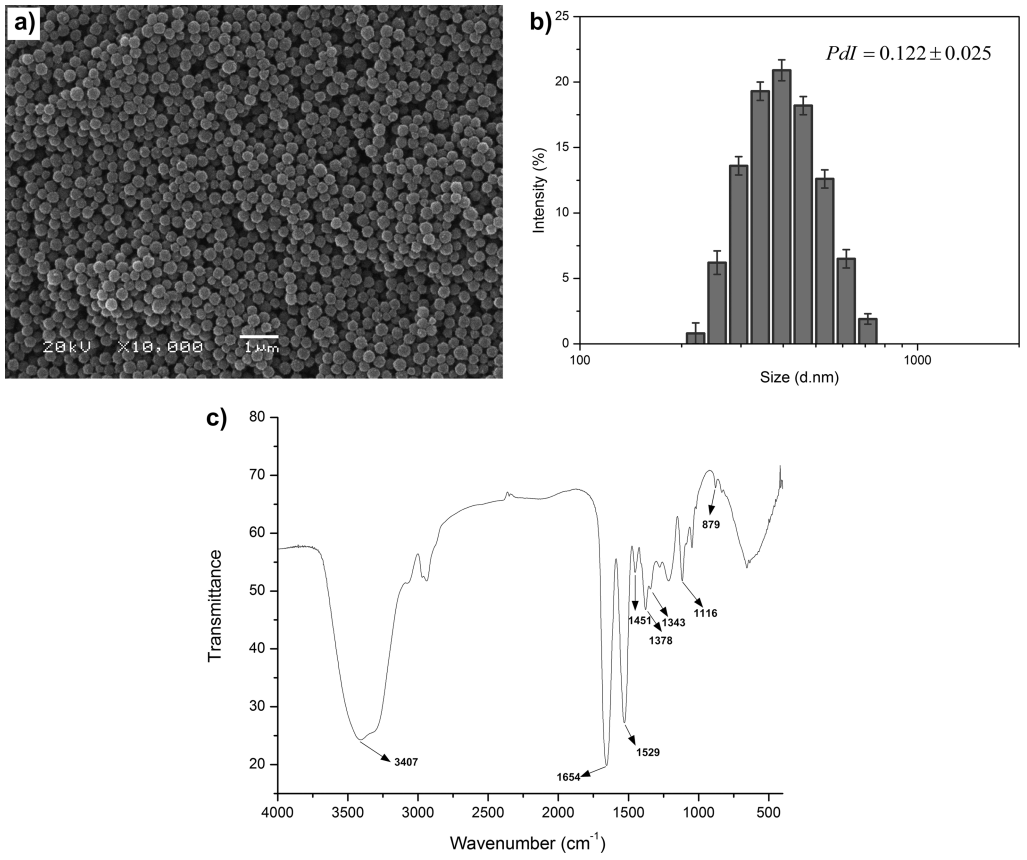

Figure 1. (a) SEM image, (b) size distribution, and (c) FT-IR spectra of P(MBA-*co*-VPBA) nanoparticles.

Table 1. δ_d, δ_p, δ_h, V, $\chi_{s,p}$, and Morphology of P(MBA-*co*-VPBA) Prepared by the PP Strategy[a]

ethanol (%)	δ_d (MPa$^{1/2}$)	δ_p (MPa$^{1/2}$)	δ_h (MPa$^{1/2}$)	V	$\chi_{s,p}$	observation
20	17.93	16.49	17.08	20.99	0.63	particle
40	17.70	15.64	17.34	25.11	0.74	coagulum
60	17.36	14.41	17.71	31.12	0.90	coagulum
80	16.81	12.44	18.30	40.72	1.19	coagulum

[a]For the polymerization system, the monomer molar ratio feed for MBA/VPBA was 6:1 and the solvent mixture was composed of ethanol and water with different volume percentages of ethanol.

To increase the loading amount of VPBA in the formed particles and to obtain simultaneously monodisperse particles, a novel mixture solvent for PP composed of water and ethanol was developed. When the volume percentage of ethanol was fixed at 20% (water/ethanol, 4:1 (v/v)), the concentration of VPBA could be increased to 0.026 mol L^{-1}. Under these conditions, submicrometer P(MBA-*co*-VPBA) particles were successfully prepared with a monomer molar ratio of MBA and VPBA of 6:1 by PP.

The morphology of P(MBA-*co*-VPBA) particles was characterized using SEM. The image revealed the formation of monodisperse submicrometer particles with spherical shape and an approximate average size of 250 nm (Figure 1a). The narrow particle size distribution was further demonstrated with the low polydispersity index (PdI) value of 0.122 ± 0.025, observed by DLS (Figure 1b). As shown in the FT-IR spectrum of submicrometer P(MBA-*co*-VPBA) particles (Figure 1c), the characteristic bands at 1378 and 1343 cm^{-1} were assigned to B−O stretching,[14,28] and those at 1451 (C−C stretching), 1116 (C−H stretching), and 879 cm^{-1} (C−H stretching) were assigned to the stretching bands of benzene in VPBA. The characteristic absorbance of the amide group of MBA segment was found at 1654 (C═O stretching), 1529 (−NH−CO− stretching), and 2047 cm^{-1} (N−H stretching), which confirmed the presence of VPBA and MBA in the particles.

Solvent-Induced Morphology Transition. We further investigated whether P(MBA-*co*-VPBA) particles could also be formed when the volume ratio of ethanol in the solvent mixture was changed. The experimental results indicated that the final product was changed from spherical to coagulum when the ethanol volume was increased from 20 to 80% in the polymerization systems (Table 1). Hansen's solubility parameters (HSPs) and Flory−Huggins theory were applied to explain such phenomenon.

According to Flory−Huggins theory[29−31] for polymer solutions, the free energy of a mixture is as follows

$$\Delta G_{mix} = n_s RT\chi_{s,p}\Phi_s + RT[n_s \ln \Phi_s + n_p \ln \Phi_p] \quad (1)$$

where $\chi_{s,p}$ is Flory's parameter, related to the interaction between solvent molecules and polymer segments, which could be further expressed by eq 2

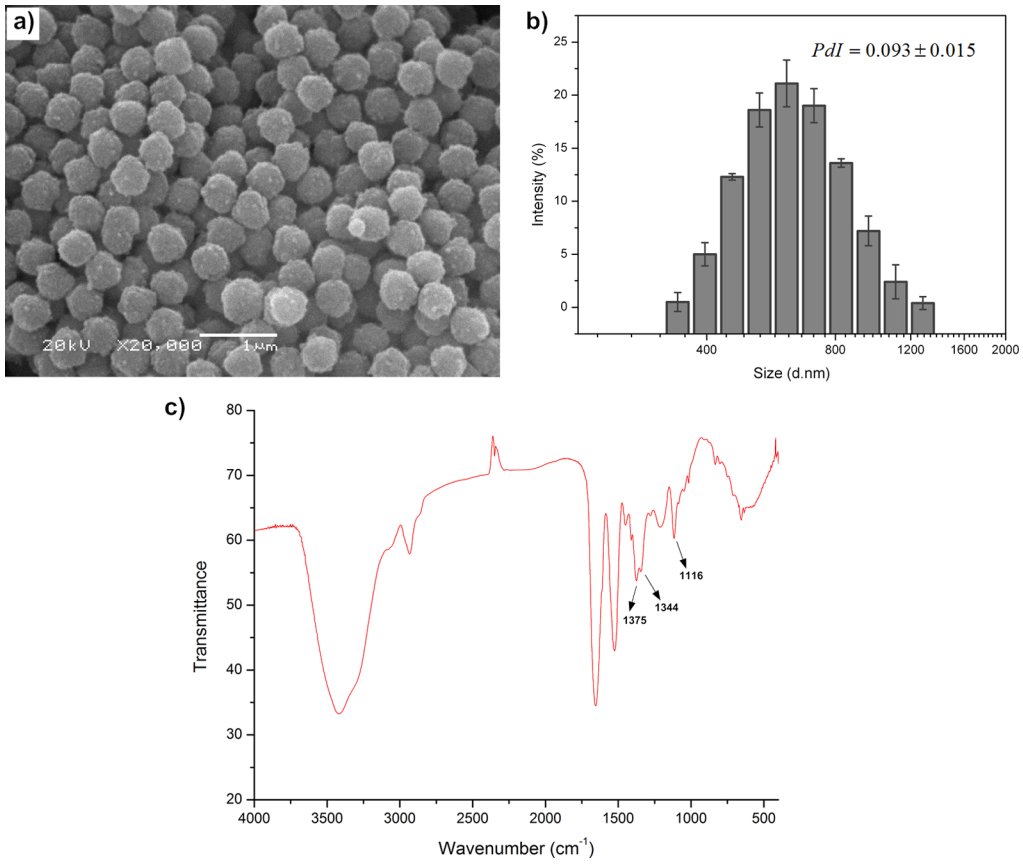

Figure 2. (a) SEM image, (b) size distribution, and (c) FT-IR spectra of P(MBA-*co*-VPBA-*co*-DVB) nanoparticles.

$$\chi_{s,p} = \left(\frac{V_s}{4RT}\right)R_{s,p}^2 \quad (2)$$

where V_s is the molecular size of the solvent and $R_{s,p}$, solubility parameter distance, is the relationship between the respective partial solubility parameter components of two materials.[19] The $R_{s,p}$ between polymer, p, and solvent, s, could be defined by eq 3

$$R_{s,p}^2 = [4(\delta_{d,p} - \delta_{d,s})^2 + (\delta_{p,p} - \delta_{p,s})^2 + (\delta_{h,p} - \delta_{h,s})^2]^{1/2} \quad (3)$$

where δ, Hansen's solubility parameters (HSPs), contributes to three parameters: dispersion, δ_p, dipole, δ_d, and hydrogen bonding, δ_h.[32,33] Additional equations related to HSPs and the calculations of HSPs are supplied in the Supporting Information.

In the nucleation step of PP, polymerization is initiated by the decomposition of initiator followed by the gradual growth of polymeric chains with the increase of the average molecular weight.[34] Once polymeric chains cannot be dissolved in the solution, the critical point ($\Delta G_{prec} = 0$) of the reaction is reached. At this critical point, the average molecular weight of the polymeric chains reaches the maximum, and the polymeric chains begin to precipitate as particles or amorphous materials (gel).[25] Therefore, there are two basic requirements for the solvent used in PP: the first is that the monomer can be dissolved in the solvent to formulate the homogeneous system, and the second is that the obtained polymer chain cannot be dissolved in the solvent when it grows to certain molecular weight, leading to its precipitation. Moreover, the average molecular weight of the polymeric chains before the critical point is dependent on the interaction between the polymeric chains and solutions, which is defined as Flory's parameter,[25] $\chi_{s,p}$. When $\chi_{s,p}$ is less than 0.5, the polymer is generally considered to be dissolube, whereas the polymer may achieve phase separation if $\chi_{s,p}$ is higher than 0.5. In the case where $\chi_{s,p}$ is higher than 0.5, the polymeric chains dissolve well when the value of the $\chi_{s,p}$ is close to 0.5, that is, the largest average molecular weight of the solvated polymeric chains will be provided at the critical point.[25,32] Therefore, $\chi_{s,p}$ further affects the product architecture that will be formed in the solvent system, such as soluble polymers (including microgels), macrogels, microspheres, or coagulum.

The HSPs and Flory's parameters, $\chi_{s,p}$, of four different solvent systems were calculated, as shown in Table 1. It was observed that spherical particles were formed when ethanol accounted for 20% in the mixture, with an $\chi_{s,p}$ of 0.63. Coagulum was formed when ethanol accounted for 40% in the mixture, with an $\chi_{s,p}$ of 0.74. Therefore, it could be deduced that the critical value of $\chi_{s,p}$ to form spherical particles or coagulum must be a certain value between 0.63 and 0.74. We set this value as Φ ($0.63 < \Phi < 0.74$). When $\chi_{s,p}$ is larger than the critical value Φ, the average molecular weight of the polymeric chains is smaller than that of polymer chains, with $\chi_{s,p}$ being smaller than Φ. According to the principle of PP, it is hard for polymer chains with a small molecular weight to form homocoagulated oligomers and then stable nuclei;[25] therefore, a networklike coagulum morphology was obtained instead of spherical particles. Another reason for this is that with the increase of ethanol the HSPs, δ_h, of the solvent mixture gradually increased. Therefore, the polymerization oligomers in mixture solvents aggregated to coagulum because of the

dx.doi.org/10.1021/am405144x | ACS Appl. Mater. Interfaces 2014, 6, 2059−2066

Table 2. *Z* Average, Zeta Potential, and $\chi_{s,p}$ of Particles Prepared by PP[a]

entry	monomer molar ratio feeds	$\chi_{s,p}$[b]	*Z*-average hydrodynamic diameter (nm)	zeta potential (mV)
1	MBA/VPBA 6:1	0.63	389.3 ± 5.0	−25.9 ± 1.1
2	MBA/VPBA/DVB 3:1:1	0.66	614.3 ± 13.3	−0.571 ± 0.045

[a]For the polymerization system, the monomer molar ratio feeds is presented and the solvent system was water/ethanol (4:1, v/v). [b]The value of $\chi_{s,p}$ is a theoretical value calculated by the Flory−Huggins model.

enhanced hydrogen-bonding interaction between ethanol and the amide group of MBA.[35] Therefore, the fact that boronic polymer particles can be formed with the highest loading amount of VPBA in the sphere by using ethanol/water (1/4, v/v) as the reaction solvent can be well-explained using HSPs and Flory−Huggins theory.

Hydrophobic Comonomers Polymerization with VPBA by the PP Strategy. Herein, VPBA was, to the best of our knowledge, for the first time, applied to prepare P(MBA-*co*-VPBA) particles by the PP strategy in the mixture solvent. To extend the general applicability of our method, another hydrophobic functional monomer, divinylbenzene (DVB), was employed to copolymerize with VPBA and MBA (Scheme 1). Under the same conditions with the PP strategy, submicrometer P(MBA-*co*-VPBA-*co*-DVB) particles were successfully prepared with varied molar ratios of monomers and cross-linkers.

The morphology of the obtained submicrometer P(MBA-*co*-VPBA-*co*-DVB) particles was characterized using SEM. As shown in Figure 2a, the particles had a relatively uniform physical shape, with a diameter of approximately 600 nm. The particle size, expressed as the apparent *Z*-average hydrodynamic diameter, was detected in water by means of DLS. The hydrodynamic diameter of P(MBA-*co*-VPBA-*co*-DVB) was 614.3 ± 13.3 nm, with a polydispersity index (PDI) of 0.093 ± 0.015, which demonstrates the good monodispersity and narrow particle-size distribution (Figure 2b). By FT-IR (Figure 2c), VPBA was demonstrated to be successfully copolymerized into such particles, as evidenced by the obvious presence of characteristic absorbance for the B−O stretching frequency at 1375 (1372) and 1344 cm^{-1}. In addition, the peak of 1116 cm^{-1}, corresponding to the characteristic absorbance of benzene rings, revealed the copolymerization of DVB in P(MBA-*co*-VPBA-*co*-DVB) particles.

According to Flory's parameter theory, when $\chi_{s,p}$ is higher than 0.5, the lower the value $\chi_{s,p}$ is, the larger the particle size will be. As shown in Table 2, both the *Z*-average hydrodynamic diameter and $\chi_{s,p}$ value of P(MBA-*co*-VPBA-*co*-DVB) particles were larger than that of P(MBA-*co*-VPBA), which is against the deductions obtained according to Flory−Huggins model. To explore this phenomenon, the zeta potential of the prepared polymer particles was further measured. Because the charges on the particle surface were basically introduced by VPBA, the P(MBA-*co*-VPBA-*co*-DVB) zeta potential close to zero (Table 2) illustrated the small amount of boronic acid on the surface, with most VPBA being inside the particles. This demonstrated that at the beginning of polymerization the reaction ratio of VPBA was faster than other monomers, making the amount of VPBA on the polymer chains of P(DVB-*co*-MBA-*co*-VPBA) larger than the feeding amount (20%). In that case, the $\chi_{s,p}$ values of the real polymeric chains was lower than the theoretical value of 0.66 calculated by the Flory−Huggins model, which is even lower than 0.63, the $\chi_{s,p}$ values of P(MBA-*co*-VPBA) in which the molar ratio of VPBA was 1:7. Therefore, according to the relation between $\chi_{s,p}$ and the average molecular weight based on the above-mentioned Flory−Huggins model, the average molecular weight of polymeric chains of P(MBA-*co*-VPBA-*co*-DVB) is larger than that of P(MBA-*co*-VPBA) at the critical point, resulting in the size of the resulting P(MBA-*co*-VPBA-*co*-DVB) particles being reasonably larger than the P(MBA-*co*-VPBA) particles.

Effect of the Format of Boronic Acid-Based Particles on Glycoprotein Enrichment. According to the principle of boronate affinity (Scheme 1b), polymer particles can capture and release glycoproteins once the pH of the buffer changes from basic to acidic[5,6] once boronic acid groups have been successfully functionalized on the surface of the particles. To evaluate the enrichment capacity of VPBA-containing polymer particles toward glycoprotein, a protein mixture consisting of glycoprotein, HRP (M_w 43 367.5 Da), and nonglycoprotein, BSA (M_w 66 786.6 Da) at a ratio (m/m) of 1:1 and at a concentration of 50 ng μL^{-1} was incubated with two kinds of prepared VPBA-containing polymer particles, respectively, and the captured proteins were further analyzed by MALDI-TOF MS.

As shown in Figure 3a, without enrichment, the peaks representing HRP and BSA could be observed in the direct

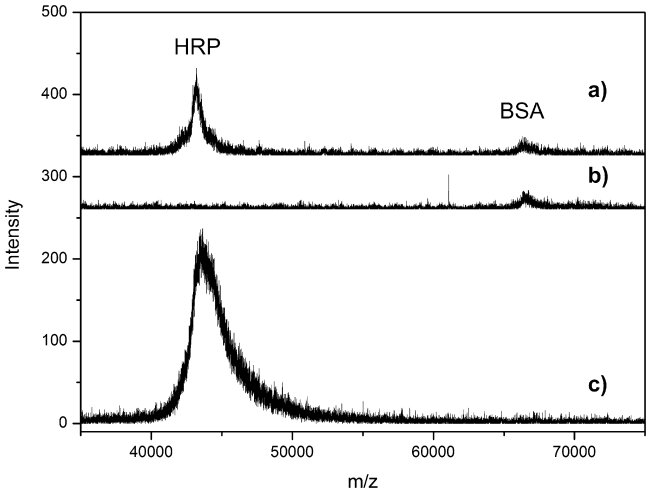

Figure 3. MALDI-TOF mass spectra of HRP and BSA mixture at a ratio of 1:1 (m/m, 50 ng μL^{-1}): (a) before enrichment, (b) supernatant, and (c) eluent after enrichment with P(MBA-*co*-VPBA).

analysis of the protein mixture. However, after enrichment with P(MBA-*co*-VPBA) nanoparticles, the signal of HRP almost disappeared in the supernatant (Figure 3b). Meanwhile, the signal-to-noise (S/N) ratio of HRP in the eluent was improved by approximately 2.5-fold compared to that from the direct analysis of the protein mixture, and BSA could not be detected (Figure 3c). Such results demonstrate the selective-enrichment ability of our prepared P(MBA-*co*-VPBA) nanoparticles. However, for P(MBA-*co*-VPBA-*co*-DVB) particles, both glycoprotein and nonglycoprotein were eluted directly without any affinity in basic media (Figure S1).

To explain such phenomena, the zeta potential of VPBA-containing polymeric particles in neutral medium was measured. As shown in Table 2, the surface charge of P(MBA-*co*-VPBA) particles was −25.9 ± 1.1 mV, which is larger than that of P(MBA-*co*-VPBA-*co*-DVB). Because MBA cannot introduce any charge in the neutral medium, the obtained zeta potential of P(MBA-*co*-VPBA) particles could be totally attributed to the existence of boronic acid groups of VPBA on the particle surface, which play an important role in glycoprotein enrichment. However, no recognition capacity toward glycoproteins was observed with P(MBA-*co*-VPBA-*co*-DVB) particles, with the zeta potential closed to zero, because of the less functional boronic acid groups of VPBA on the particle surface. On the basis of the above-mentioned deduction from the standpoint of the Flory−Huggins model, this was because that the reaction ratio of VPBA was faster than that of MBA or DVB in P(MBA-*co*-VPBA-*co*-DVB) particles, resulting in most of the VPBA being consumed in the process of core formation and little boronic acid being introduced onto the surface of the particles.

Therefore, the choice of a suitable solvent system and comonomers to obtain an appropriate VPBA reaction rate in the precipitation process is a prerequisite to prepare VPBA-based polymer particles that ensure boronic acid functionalization on their surface and thus present good glycoprotein recognition ability.

On the basis of the Flory−Huggins model, monomers such as *N*-vinylcaprolactam (NVCL), ethyleneglycol dimethacrylate (EGDMA), and *N*-isopropylacrylamide (NIPA) could be chosen to replace DVB to formulate the polymer particles by precipitation polymerization. Among the proposed monomers in theory, the P(MBA-*co*-VPBA-*co*-NVCL) particles were prepared.[36] The $\chi_{s,p}$ of P(MBA-*co*-VPBA-*co*-NVCL) was calculated to be 2.81, with the feed molar ratio of MBA, VPBA, and NVCL as 1:1:6 in the water solvent. The particle could be formulated because the value of $\chi_{s,p}$ is higher than 0.5, and the size of particle was smaller than that of P(MBA-*co*-VPBA) because of the higher $\chi_{s,p}$ value than that of P(MBA-*co*-VPBA), corresponding to the Flory−Huggins model. Furthermore, the particles also have an effect on the glucose response. This case further demonstrated that other monomer could displace the DVB monomer to obtain glucose-responsive nanoparticles based on the Flory−Huggins model. Therefore, the Flory−Huggins model prediction might provide guidance for synthesizing functionalized polymer particles by using the precipitation−polymerization method.

Evaluation of P(MBA-*co*-VPBA) Particles on Glycoprotein Recognition. To investigate the adsorption capacity of P(MBA-*co*-VPBA) particles for glycoproteins, the adsorption isotherms was studied with an HRP concentration ranging from 0.1 to 1 mg mL^{-1}. As shown in Figure S2, the saturation of adsorption for HRP tended to reach an adsorption plateau at 0.7 mg mL^{-1}. The saturation adsorption capacity for HRP was estimated to be 100.22 ± 8.60 mg g^{-1}, higher than that of the boronic acid-functionalized material prepared by multistep modifications,[37] indicating that particles prepared by one-pot PP have a high adsorption capacity for glycoprotein. On the contrary, the adsorption capacity towards nonglycoproteins was much less, with the maximum adsorption capacity being lower than 3 mg g^{-1} for BSA, indicating that P(MBA-*co*-VPBA) had a low nonspecific adsorption for nonglycoproteins because of the improved hydrophilicity with MBA as the monomer.

The reproducibility for glycoprotein enrichment by P(MBA-*co*-VPBA) was further studied with the mixture of HRP and BSA as the sample. The eluents from three parallel enrichments were analyzed by MALDI-TOF MS. As shown in Figure S3, after enrichment, only HRP was observed in the eluent, with similar peak profiles in the three runs. Furthermore, the relative quantity of protein in the eluents was measured by HPLC at regular intervals, and the RSD of the peak height of HRP was 6.65%. All of these results demonstrate the good reproducibility of glycoprotein enrichment with P(MBA-*co*-VPBA) nanoparticles.

On the basis of the principle that the specific binding between phenylboronic acid and the cis-diol of the glycoprotein is reversible in basic/acidic media, P(MBA-*co*-VPBA) particles were repeatedly used for glycoprotein enrichment. As shown in Figure S4, the peaks representing HRP and BSA could be observed in the direct analysis of the protein mixture. Meanwhile, HRP alone was observed in the eluent after the first adsorption−desorption cycle, which was the same after up to five cycles, as shown in Figure S4. Such results demonstrate that our prepared P(MBA-*co*-VPBA) nanoparticles can be used at least five times without the loss of glycoprotein-recognition capacity.

Application of P(MBA-*co*-VPBA) Particles in Real Sample Analysis. To evaluate the capability and selectivity of P(MBA-*co*-VPBA) towards the analysis of glycoproteins in real samples, egg white was employed as the sample. As shown in Figure 4, by SDS-PAGE analysis, before enrichment, several

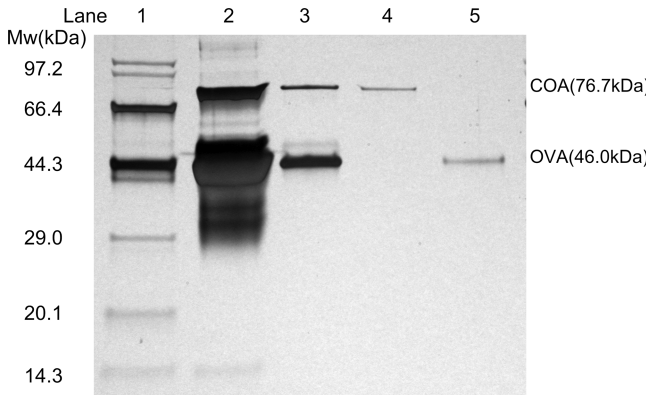

Figure 4. SDS-PAGE analysis of egg white with and without treatment by P(MBA-*co*-VPBA). Lane 1, marker; 2, egg white without treatment (1.5 μg); 3, egg white after treatment; 4, COA standard (100 ng); and 5, OVA standard (100 ng).

bands, indicating various proteins existed in egg white, appeared in lane 2. After treated by P(MBA-*co*-VPBA), two protein bands located at ∼76.7 and ∼46 kDa emerged in the eluted fraction (lane 3). They represent the glycoproteins conalbumin (COA), aligned to the location of pure COA in lane 4, and ovalbumin (OVA), aligned to the location of pure OVA in lane 5. The clear glycoprotein bands and extremely clean nonglycoprotein background in SDS-PAGE further revealed the good capability and selectivity of such smart polymer particles for glycoprotein recognition in real biological samples.

4. CONCLUSIONS

A one-pot strategy to prepare monodisperse boronic acid-containing submicrometer polymer particles by a precipitation

polymerization technique in a novel ethanol/water solvent system was developed. The particle formation in different solvent systems was discussed on the basis of the Flory model. Furthermore, particle diameters or surface properties related to the glycoprotein-recognition capacity of the particles was also explained by the same model. Our prepared P(MBA-*co*-VPBA) nanoparticles were of good hydrophilicity and high boronic acid group density on the surface, which favored the specific recognition of glycoproteins. Moreover, the particle synthesis by such a strategy was facile, time-saving, and, importantly, without dispersant disturbance. All of the results indicate that the PP strategy together with Flory−Huggins model verification might provide a perspective and guidance for synthesizing boronic acid-functionalized polymer particles with high specificity toward glycoprotein recognition.

■ ASSOCIATED CONTENT

Supporting Information

Equations related to HSPs and the calculations of HSPs, MALDI-TOF mass spectra of P(MBA-*co*-VPBA-*co*-DVB) particles for glycoprotein recognition, and adsorption isotherm of P(MBA-*co*-VPBA) towards HRP and BSA. This material is available free of charge via the Internet at http://pubs.acs.org.

■ AUTHOR INFORMATION

Corresponding Author

*E-mail: lihuazhang@dicp.ac.cn.

Notes

The authors declare no competing financial interest.

■ ACKNOWLEDGMENTS

This work was supported by the National Basic Research Program of China (2012CB910601 and 2013CB911201), the National Natural Science Foundation (21005078, 21190043, and 21005079), the Creative Research Group Project by NSFC (21321064), the National High Technology Research and Development Program of China (2012AA020202), and the Analytical Method Innovation Program of MOST (2012IM030900).

■ REFERENCES

(1) Kim, H.; Kang, Y. J.; Kang, S.; Kim, K. T. *J. Am. Chem. Soc.* **2012**, *134*, 4030−4033.
(2) Roy, D.; Sumerlin, B. S. *ACS Macro Lett.* **2012**, *1*, 529−532.
(3) Uğuzdoğan, E.; Denkbaş, E. B.; Tuncel, A. *Macromol. Biosci.* **2002**, *2*, 214−222.
(4) De Guzman, J. M.; Soper, S. A.; McCarley, R. L. *Anal. Chem.* **2010**, *82*, 8970−8977.
(5) James, T. D.; Sandanayake, K. R. A. S.; Shinkai, S. *Angew. Chem., Int. Ed. Engl.* **1996**, *35*, 1910−1922.
(6) Nishiyabu, R.; Kubo, Y.; James, T. D.; Fossey, J. S. *Chem.Commun.* **2012**, *47*, 1106−1123.
(7) Frasconi, M.; Tel-Vered, R.; Riskin, M.; Willner, I. *Anal. Chem.* **2010**, *82*, 2512−2519.
(8) Liang, L.; Liu, Z. *Chem.Commun.* **2011**, *47*, 2255−2257.
(9) Zhang, L.; Xu, Y.; Yao, H.; Xie, L.; Yao, J.; Lu, H.; Yang, P. *Chem.—Eur. J.* **2009**, *15*, 10158−10166.
(10) Xu, Y.; Wu, Z.; Zhang, L.; Lu, H.; Yang, P.; Webley, P. A.; Zhao, D. *Anal. Chem.* **2008**, *81*, 503−508.
(11) Zhong, X.; Bai, H.-J.; Xu, J.-J.; Chen, H.-Y.; Zhu, Y.-H. *Adv. Funct. Mater.* **2010**, *20*, 992−999.
(12) Wu, W.; Mitra, N.; Yan, E. C.; Zhou, S. *ACS Nano* **2010**, *4*, 4831−9.
(13) Zhang, L.; Lin, Y.; Wang, J.; Yao, W.; Wu, W.; Jiang, X. *Macromol. Rapid. Commun.* **2011**, *32*, 534−9.
(14) Shen, W.-W.; Ma, C.-N.; Wang, S.-F.; Xiong, H.-M.; Lu, H.-J.; Yang, P.-Y. *Chem.—Asian J.* **2010**, *5*, 1185−1191.
(15) Pan, M.; Sun, Y.; Zheng, J.; Yang, W. *ACS Appl. Mater. Interfaces* **2013**, *5*, 8351−8358.
(16) Qu, Y.; Liu, J.; Yang, K.; Liang, Z.; Zhang, L.; Zhang, Y. *Chem.—Eur. J.* **2012**, *18*, 9056−9062.
(17) Yang, K. G.; Berg, M. M.; Zhao, C. S.; Ye, L. *Macromolecules* **2009**, *42*, 8739−8746.
(18) Sauer, R.; Turshatov, A.; Baluschev, S.; Landfester, K. *Macromolecules* **2012**, *45*, 3787−3796.
(19) Shi, Y.; Lv, H.; Lu, X.; Huang, Y.; Zhang, Y.; Xue, W. *J. Mater. Chem.* **2012**, *22*, 3889−3898.
(20) Xu, C.; Shen, X.; Ye, L. *J. Mater. Chem.* **2012**, *22*, 7427−7433.
(21) Haraguchi, N.; Nishiyama, A.; Itsuno, S. *J. Polym. Sci., Polym. Chem.* **2010**, *48*, 3340−3349.
(22) Li, K.; Stöver, H. D. H. *J. Polym. Sci., Polym. Chem.* **1993**, *31*, 3257−3263.
(23) Wang, J.; Cormack, P. A.; Sherrington, D. C.; Khoshdel, E. *Angew. Chem., Int. Ed.* **2003**, *42*, 5336−5338.
(24) Wisniewski, J. R.; Zougman, A.; Nagaraj, N.; Mann, M. *Nat. Methods* **2009**, *6*, 359−362.
(25) Medina-Castillo, A. L.; Fernandez-Sanchez, J. F.; Segura-Carretero, A.; Fernandez-Gutierrez, A. *Macromolecules* **2010**, *43*, 5804−5813.
(26) Frank, R. S.; Downey, J. S.; Yu, K.; Stover, H. D. H. *Macromolecules* **2002**, *35*, 2728−2735.
(27) *Polymer Handbook*, 4th ed.; Bradrup, J., Immergut, E. H., Grulke, E. A., Abe, A., Bloch, D. R., Eds.; Wiley-Interscience: New York, 1999; Vol. *7*, pp 683−689.
(28) Voss, K. F.; Foster, C. M.; Smilowitz, L.; Mihailović, D.; Askari, S.; Srdanov, G.; Ni, Z.; Shi, S.; Heeger, A. J.; Wudl, F. *Phys. Rev. B* **1991**, *43*, 5109−5118.
(29) Flory, P. J. *Principles of Polymer Chemistry*, 5th ed.; Cornell University Press: Ithaca, NY, 1992; Vol. *12*, pp 507−527.
(30) Flory, P. J. *J. Am. Chem. Soc.* **1965**, *87*, 1833−1838.
(31) Shultz, A. R.; Flory, P. J. *J. Am. Chem. Soc.* **1952**, *74*, 4760−4767.
(32) Hansen, C. M. *Hansen Solubility Parameters: A User's Handbook*, 2nd ed.; CRC Press: Boca Raton, FL, 2007; Vol. *1*, pp 7−22.
(33) Lawson, D. D. *Appl. Energy* **1980**, *6*, 241−255.
(34) Odian, G. *Principles of Polymerization*, 4th ed.; Wiley Interscience: Hoboken, NJ, 2004.
(35) Liu, G.; Yang, X.; Wang, Y. *Polym. Int.* **2007**, *56*, 905−913.
(36) Bitar, A.; Fessi, H.; Elaissari, A. *J. Biomed. Nanotechnol.* **2012**, *8*, 709−719.
(37) Li, Y.; Hong, M.; Miaomiao; Bin, Q.; Lin, Z.; Cai, Z.; Chen, G. *J. Mater. Chem. B* **2013**, *1*, 1044−1051.